

Sub-diffraction-limit imaging based on the topographic contrast of differential confocal microscopy

Chau-Hwang Lee, Hui-Yu Chiang, and Hong-Yao Mong

Institute of Applied Science and Engineering Research, Academia Sinica, 128 Academia Road, Section 2, Nankang, Taipei 115, Taiwan

Received January 17, 2003

Using the nanometer depth sensitivity of differential confocal microscopy, we detect surface features of lateral dimensions smaller than the diffraction limit without fluorescence labeling. The lateral resolution of the topographic images is further enhanced by a maximum-likelihood estimation algorithm. Based on the comparison of signal and noise at high spatial frequency, we estimate the best lateral resolution of the enhanced images to be 0.15λ . In addition, on composite samples this technique can simultaneously display sub-diffraction-limit topographic features and reflectivity heterogeneity. © 2003 Optical Society of America

OCIS codes: 100.3020, 100.6640, 180.0180.

In the past decade the resolution of far-field fluorescence microscopy has been successfully improved to the sub-diffraction-limit regime. For example, by use of image-restoration algorithms along with precise measurements of the point-spread function (PSF), far-field optical microscopy can provide model images close to the objects with resolution much better than the diffraction limit.^{1,2} The resolution of far-field fluorescence microscopy can also be enhanced by modification of the PSF, such as quenching the fluorescence with stimulated emission with ultrashort laser pulses.³ With the wave front of the quenching pulses modified by phase plates, a focal spot of axial extent $\lambda/23$ has been demonstrated.⁴ Structured illumination has also been used to bring signals of higher spatial frequency into a conventional imaging system and hence to enhance the lateral resolution beyond the diffraction limit.^{5,6} Moreover, by spectrally selecting a single molecule with high-resolution laser spectroscopy, one can even resolve a single molecule with lateral resolution as high as 40 nm in the far field.⁷

To achieve sub-diffraction-limit resolution, a primary requirement is obtaining sufficient contrast from objects that are smaller than a wavelength. Most of the existing methods employ the high-contrast signal provided by fluorescent dyes or scattering particles. Nevertheless, dye labeling is not always appropriate for biological specimens because of its potentially poisonous effects. For other samples, such as semiconductor devices, contaminative labeling is usually prohibited. For samples that cannot be labeled with dyes, scanning electron microscopy (SEM) serves as the workhorse for inspecting submicrometer features. However, SEM requires a conductive surface for good contrast and must operate in a vacuum. Scanning probe microscopy is also widely employed to observe features smaller than optical resolution. But the risk of scratching sample surfaces with the probes is not favorable. A far-field imaging technique with sub-diffraction-limit resolution that does not use fluorescence labeling is thus desirable for fast and nonintrusive diagnosis of surface features.

Without fluorescent dyes and scattering particles one must employ new mechanisms to produce sufficiently high contrast. Recently an imaging ellipsometer was employed to characterize subwavelength

surface features by the polarization-ratio signal.⁸ The measurements had 10-nm accuracy on isolated lines wider than 100 nm. In this Letter we propose superresolution far-field microscopy with the topographic contrast provided by differential confocal microscopy (DCM). DCM has been demonstrated to have 2-nm depth resolution on surfaces with homogeneous reflectivity.⁹ For practical samples such as microelectronic circuits, the aspect ratio is usually 0.1–10; therefore nanometer depth resolution implies a sensitivity high enough to detect features of lateral dimensions of approximately tens of nanometers. With sufficient contrast the lateral resolution of DCM images can be improved beyond the diffraction limit by restoration algorithms.

The setup and working principle of DCM have been described in our previous publications.^{9,10} In brief, the sample surface is placed approximately half a confocal parameter from the focal plane along the optical axis of a confocal microscope, where the confocal signal is so sensitive to the axial displacement that nanometer height variations result in a high-contrast signal. In this work we use a 532-nm solid-state laser as the light source and an electro-optical stabilizer to reduce the intensity fluctuation to less than 0.05%. The DCM signal is digitized by a 16-bit analog-to-digital converter. Lateral scanning is performed by a two-axis closed-loop piezoelectric-transducer-driven stage with 1-nm positioning repeatability. The probe is a 0.95-numerical-aperture, 100 \times objective. The Rayleigh resolution limit of this objective is 340 nm. The PSF of this setup is characterized by the use of a 100-nm latex bead placed on a glass substrate as the sample. The bead and the substrate are coated with 15-nm-thick gold to have uniform reflectivity. With DCM we measure the lateral FWHM of the bead signal to be 400 nm.

Image restoration is performed by a maximum-likelihood estimation (MLE) algorithm with the iteration kernel¹¹

$$g_{k+1}(\mathbf{x}) = g_k(\mathbf{x}) \int_{\mathbf{y}} \left[\frac{h(\mathbf{x} - \mathbf{y})}{\int_{\mathbf{x}} h(\mathbf{y} - \mathbf{x}) g_k(\mathbf{x}) d\mathbf{x}} \right] m(\mathbf{y}) d\mathbf{y}, \quad (1)$$

where g is the estimated model image, h is the PSF, and m is the measured raw image. \mathbf{x} and \mathbf{y} represent

the coordinate vectors of the object and image spaces, respectively. The superresolution capability of such a MLE restoration algorithm has been theoretically and experimentally verified by Conchello,¹² showing that the passband of an optical image can be extended and the restored high-spatial-frequency image is not artificial. In addition, compared with other image-restoration algorithms, the MLE algorithm is not only easy to implement but also more robust against noise.¹³ In this work the restorations are performed on a personal computer equipped with a 1.0-GHz AMD Athlon processor and a 512-Mbyte RAM. The restored image is evaluated by the *I*-divergence difference measure.¹⁴ The iteration stops when the *I*-divergence reaches 10^{-4} .

The smallest resolvable dimension of the MLE restoration is limited by noise from mechanical vibration, quantization error of the analog-to-digital converter, and intensity fluctuation of the light source. Since these noises are independent of the scale of the image, at high spatial frequency the signal can be smaller than a noise floor. It has been pointed out that MLE can recover only the image components of spatial frequency smaller than a certain value at which the spectrum of the signal crosses the noise level.¹⁵ This crossover frequency sets the resolution limit. To estimate the resolution limit of the restored DCM images, we fabricate a gold line of 140-nm width and 80-nm height as a specimen [Fig. 1(a)], then use its DCM image for the comparison of signal and noise spectra. Figure 1(b) is the DCM image, which can be regarded as the line-spread function. Figure 1(c) shows the restored image. The cross-sectional profiles before and after the restoration process are compared in Fig. 1(d), showing that the width is decreased by a factor of 2.9. To find the resolution limit of restoration, we compare the spectrum of a cross-sectional profile of Fig. 1(b) and that of noise measured on the blank area of the same sample. As shown in Fig. 1(e), the noise is higher than the signal at a spatial frequency of $\sim 12.2 \mu\text{m}^{-1}$, corresponding to a lateral dimension of 82 nm. Therefore the highest lateral resolution of the sub-diffraction-limit image obtained with our setup can be nearly 80 nm, or 0.15λ .

Figure 2 shows the restoration result by use of a 2160-lines/mm wafflelike pattern (Ted Pella, 607-AFM) as the sample. This sample is a non-conductive calibration standard for atomic force microscopes. The lines are 150–180 nm wide and 30–40 nm high. With a 550-nm incoherent light source and an ordinary optical microscope equipped with a 0.95-numerical-aperture objective, the pattern is invisible, as shown in Fig. 2(a). However, with DCM we can detect the lines at diffraction-limited resolution with high contrast. Figure 2(b) shows the restored DCM image. Away from the intersections we measure the linewidths to be 170–200 nm in Fig. 2(b). The comparison between Figs. 2(a) and 2(b) demonstrates the improvement in the resolving power of far-field optical microscopy by a combination of DCM and MLE restoration.

Figure 3 shows images of gold electrodes on a silicon surface.¹⁶ The height of these electrodes is 40 nm.

We coat the whole surface with 15-nm gold film and then use SEM to observe the details, as shown in Fig. 3(a). There are two types of electrodes: The longer are ~ 100 nm wide, and the shorter are ~ 130 nm wide. The smallest gaps between the long electrodes are ~ 90 nm. Figure 3(b) shows the restored DCM image. The long and short electrodes are distinguishable in this image. We also note that gaps smaller than 100 nm are resolvable with slightly exaggerated separations.

For samples with additional contrast from different reflectivities of the composing materials, the technique presented here can produce images with much clearer information than ordinary far-field optical microscopy. Figure 4 shows a trisquare pattern etched on silicon. The depth of the etched area is 180 nm measured by an

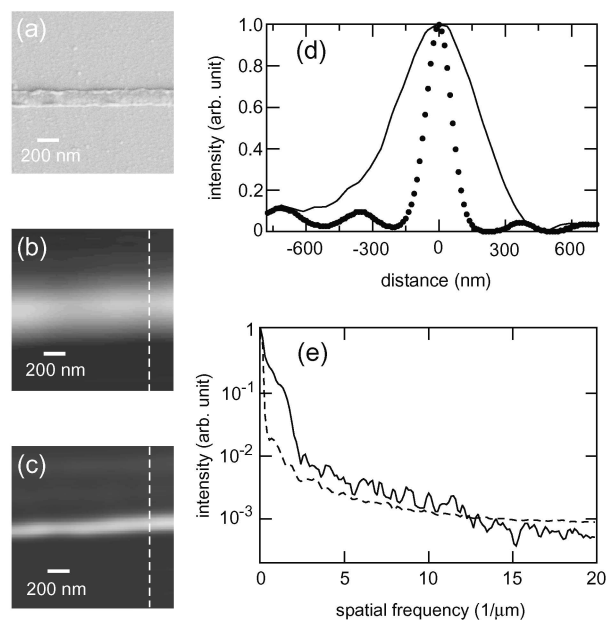


Fig. 1. Images and spectrum of a 140-nm-wide, 80-nm-high gold line. (a) SEM image. (b) Raw image obtained by DCM (120×120 pixels). (c) Restored DCM image after 745 iterations. The restored linewidth is correctly 140 nm. (d) Solid curve, cross-sectional profile of (b) at the position indicated in (b) by a dashed line. Dotted curve, cross-sectional profile of (c). After restoration the FWHM is decreased by a factor of 2.9. (e) Solid curve, spectrum of the cross-sectional profile in (b). Dashed curve, noise spectrum. The noise intensity crosses the signal at a spatial frequency of $12.2 \mu\text{m}^{-1}$.

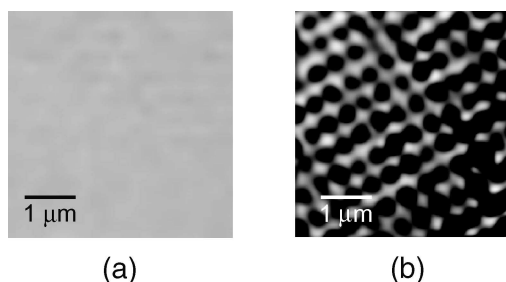


Fig. 2. Images of a 2160-lines/mm wafflelike pattern. (a) Image obtained by ordinary optical microscopy. (b) Restored DCM image after 166 iterations (400×400 pixels).

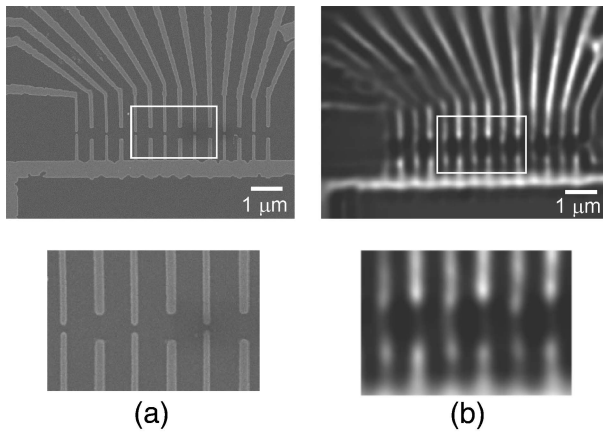


Fig. 3. Images of 40-nm-high gold electrodes. (a) SEM image. The long electrodes are 100 nm wide, and the short ones are 130 nm wide. (b) Restored DCM image after 617 iterations (374×270 pixels). The bottom row shows magnified images of the region enclosed by rectangles in the upper row. In (b) the bottom image was doubly resampled for better visibility.

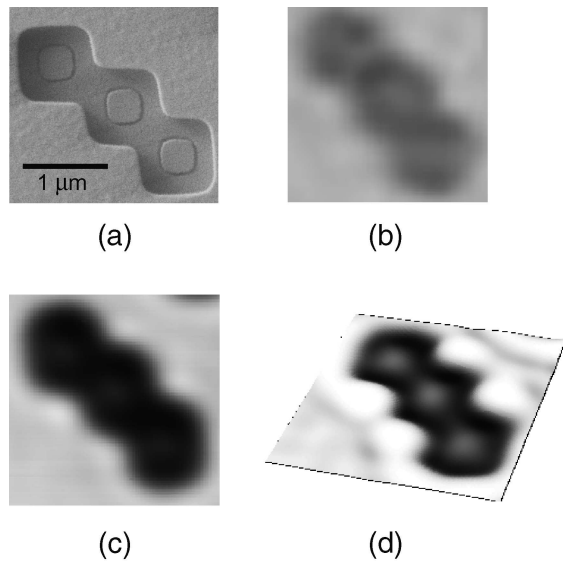


Fig. 4. Images of a trisquare pattern etched on silicon. (a) SEM image. The smaller squares inside are made of gold film. (b) Ordinary optical microscope image. (c) DCM raw image (250×250 pixels). (d) Surface plot of the restored DCM image after 290 iterations.

atomic force microscope. There are three gold squares inside the etched area. The side length of each gold square is 310 nm. With an ordinary optical microscope we obtained the image in Fig. 4(b), in which the etched region is visible, but the outline is severely blurred. Moreover, although the gold squares have higher reflectivity, they are still invisible because they are smaller than the resolution limit. Nevertheless,

with DCM and image restoration we obtain a surface plot as shown in Fig. 4(d). The three gold squares are clearly resolved with correct positions and shapes. The boundary of the etched trisquare is also apparent. The two types of information are difficult to obtain from the far-field observation in Fig. 4(b).

In summary, we have demonstrated the sub-diffraction-limit imaging capability of DCM by use of a MLE algorithm to restore the raw images. The high contrast required for image restoration is provided by the nanometer depth sensitivity of DCM. With a 532-nm solid-state laser as the light source and power fluctuation smaller than 0.05%, the noise is smaller than the signal for spatial frequencies lower than $12.2 \mu\text{m}^{-1}$. Therefore the highest lateral resolution can be ~ 80 nm, or 0.15λ . With this technique we observed a nonconductive specimen of 150–180-nm linewidth and gold electrodes nearly 100 nm wide. This technique can also display submicrometer features of different reflectivities. This method can serve as a convenient and economical complement to SEM for diagnosis in modern semiconductor and nanotechnology industries.

We thank the National Science Council of Taiwan for the financial support of this research project (contract NSC 90-2215-E-001-001). C.-H. Lee's e-mail address is cleeh@gate.sinica.edu.tw.

References

1. W. A. Carrington, R. M. Lynch, E. D. W. Moore, G. Isenberg, K. E. Fogarty, and F. S. Fay, *Science* **268**, 1483 (1995).
2. M. Schrader, S. W. Hell, and H. T. M. van der Voort, *Appl. Phys. Lett.* **69**, 3644 (1996).
3. T. A. Klar and S. W. Hell, *Opt. Lett.* **24**, 954 (1999).
4. M. Dyba and S. W. Hell, *Phys. Rev. Lett.* **88**, 163901 (2002).
5. M. G. L. Gustafsson, *J. Microsc.* **198**, 82 (2000).
6. J. T. Frohn, H. F. Knapp, and A. Stemmer, *Proc. Natl. Acad. Sci. USA* **97**, 7232 (2000).
7. A. M. van Oijen, J. Köhler, J. Schmidt, M. Müller, and G. J. Brakenhoff, *J. Opt. Soc. Am. A* **16**, 909 (1999).
8. Q. Zhan and J. R. Leger, *Opt. Lett.* **27**, 821 (2002).
9. C.-H. Lee and J. Wang, *Opt. Commun.* **135**, 233 (1997).
10. C.-W. Tsai, C.-H. Lee, and J. Wang, *Opt. Lett.* **24**, 1732 (1999).
11. See, for example, G. M. P. van Kempen, H. T. M. van der Voort, J. G. J. Bauman, and K. C. Strasters, *IEEE Eng. Med. Biol. Mag.* **15**, 76 (1996).
12. J.-A. Conchello, *J. Opt. Soc. Am. A* **15**, 2609 (1998).
13. J. Markham and J.-A. Conchello, *J. Opt. Soc. Am. A* **18**, 1062 (2001).
14. I. Csizsár, *Ann. Stat.* **19**, 2033 (1991).
15. D. L. Snyder, M. I. Miller, L. J. Thomas, Jr., and D. G. Politte, *IEEE Trans. Med. Imaging* **6**, 228 (1987).
16. We thank C.-D. Chen of the Institute of Physics, Academia Sinica, for providing this sample.